Ocean Engineering 160 (2018) 168–180

Contents lists available at ScienceDirect

Ocean Engineering

journal homepage: www.elsevier.com/locate/oceaneng

Nonlinear Model Predictive Control for trajectory tracking and collision avoidance of underactuated vessels with disturbances☆

Mohamed Abdelaal *, Martin Fränzle, Axel Hahn

Ammerländer Heerstr, 114-118, 26129, Oldenburg, Germany

ARTICLE INFO

Keywords:
Nonlinear model predictive control (NMPC)
Nonlinear disturbance obersver (NDO)
Collision avoidance
Trajectory tracking
Underactuated vessel

ABSTRACT

This paper presents a combined Nonlinear Model Predictive Control (NMPC) for position and velocity tracking of underactuated surface vessels, and collision avoidance of static and dynamic objects into a single control scheme with sideslip angle compensation and environmental disturbances counteraction. A three-degree-of-freedom (3-DOF) dynamic model is used with only two control variables: namely, surge force and yaw moment. External environmental forces are considered as constant or slowly varying disturbances with respect to the inertial frame, and hence nonlinear for the body frame of the vessel. Nonlinear disturbance observer (NDO) is used to estimate these disturbances in order to be fed into the prediction model and enhance the robustness of the controller. A nonlinear optimization problem is formulated to minimize the deviation of the vessel states from a time varying reference generated over a finite horizon by a virtual vessel. Sideslip angle is considered in the cost function formulation to account for tracking error caused by the transverse external force in the absence of sway control force. Collision avoidance is embedded into the trajectory tracking control problem as a time-varying nonlinear constraint of position states to account for static and dynamic obstacles. MATLAB simulations are used to assess the validity of the proposed technique.

1. Introduction

Path following techniques of vessels have gained a lot of interest from both academia and industry; specially for the future expectations of using commercial autonomous vessels or adding an autopilot to assist the crew. To make these techniques practical, collision avoidance should be integrated in the control problem to guarantee safe maneuvering during the trip. Collision risk is increased in the presence of external forces such as those induced by wind and waves. Motivated by these requirements, surface vessels should be able to keep the planned trajectory, while avoiding collision of nearby objects and counteraction external disturbances. The challenge is increased for underactuated surface vessels which are usually equipped with two independent aft thrusters or with one main aft thruster and a rudder, and hence have only two control variables; namely surge force and yaw moment.

In recent years, trajectory tracking has been studied using various control techniques. For instance, Dynamic Surface Control (DSC) technique is used in (Chwa, 2011) for global tracking of underactuated vessel in a modular way that cascaded kinematic and dynamic linearizations can be achieved. In (Peng et al., 2013; Wang et al., 2014), an adaptive form of DSC is used for formation control of autonomous surface vehicles (ASVs) moving in a leader-follower formation under ocean disturbances. In (Kahveci and Ioannou, 2013), an automatic adaptive steering control design for full-actuated vessels is presented. The adaptive law is combined with a control design including a linear quadratic controller (LQR) and a Riccati based anti-windup compensator. The controller also takes into consideration input constraints, wind and wave effects, and parametric uncertainty. In (Dong et al., 2015), a trajectory tracking problem is addressed for a 3-DOF underactuated Unmanned Surface Vessel (USV) using a state feedback based backstepping control algorithm with relaxed persistent exciting (PE) conditions of yaw velocity. In (Jiang and Nijmeijer, 1999), a recursive technique is presented for trajectory tracking of nonholonomic systems by the means of backstepping, and is demonstrated by simulating an articulated vehicle and a knife edge system. In (Do and Pan, 2004), a methodology for designing state and output feedback controller is presented by means of Lyapunov's direct method and backstepping after model transformation to Serret-Frenet frame. Although the aforementioned techniques give good trajectory tracking results, collision avoidance of nearby objects is not addressed.

Model Predictive Control (MPC) has got attention for trajectory

☆ This research is supported by the State of Lower Saxony as part of the project Critical Systems Engineering for Socio-Technical Systems (CSE).

* Corresponding author.
E-mail address: mohamed.abdelaal@uni-oldenburg.de (M. Abdelaal).

https://doi.org/10.1016/j.oceaneng.2018.04.026
Received 19 May 2016; Received in revised form 19 December 2017; Accepted 8 April 2018
Available online 27 April 2018
0029-8018/

tracking control problems because of its systematic ability to handle physical constraints of the system (Künhe et al., 2005). In (Guerreiro et al., 2014), NMPC is used for trajectory tracking of a full actuated autonomous surface craft (ASC) in the presence of constant ocean currents. In (Yan and Wang, 2012), MPC is applied for tracking problem of underactuated surface vessels, employing the affine property of the system model. The kinematic is simplified by applying frame transformation to make positions independent of the choice of the inertial frame. Nonlinear functions of the system are evaluated using optimal states obtained at the previous instant which leads to significant numerical errors for large horizons (Mayne, 1016). In (Abdelaal et al., 2015), NMPC is used for trajectory tracking of an underactuated vessels employing direct multiple shooting technique that leads to less numerical error. The aforementioned MPC approaches do not cater for collision avoidance.

Conventionally, collision avoidance is treated as a controller independent planning problem that might not be achievable by the controller and hence degrades the safety of the vessel (Wang et al., 1016). For instance, an evolutionary algorithm is presented in (Smierzchalski, 1999) to find a safe and optimal trajectory of surface vessels in a well known environment by using the vessel's kinematic model. A more sophisticated evolutionary approach is presented in (Szlapczynski, 2011, 2012; Szlapczynski and Szlapczynska, 2012) by adding specialized operators to shape the convergence of the optimization. In (Zhuo, 2014), a fuzzy logic approach is presented for collision avoidance of large ships by formulating the problem into an optimization problem and solving it using a particle swarm algorithm. Fuzzy-neural inference network is also used in (Liu and Shi, 2005) for ship collision avoidance. In (Wang et al., 2017a), collision avoidance is achieved in two steps: a path planning collision avoidance, and an MPC for following the generated path after linearizing the dynamics of the vessel. In (Wang et al., 2017b), a collision avoidance dynamic support system is presented where a mathematical model of ship maneuvering motion and a PID heading controller are employed as well as dynamic calculation model of collision avoidance parameter. A graph-theoretic solution on an appropriately-weighted directed graph representation of the navigation area is presented in (Ari et al., 2013). The graph is obtained via 8-adjacency integer lattice discretization and utilization of the A^* algorithm. Although the aforementioned techniques demonstrate collision avoidance, they either simplify or ignore the dynamics of the vessel, and the effect of external environmental forces.

Recently, control techniques have been developed to include collision avoidance as an objective while designing the controllers. In (Wang and Ding, 2014), MPC is used for the tracking and formation problem of multiagent linear systems with collision avoidance as a constraint for the optimization problem. In (Alrifaee et al., 2014), a centralized MPC is used for collision avoidance of networked vehicles by successively linearizing the nonlinear prediction model using Taylor series. In (Wang et al., 1016), an MPC technique is applied for the nonlinear model of kinematically redundant space robot to approach an un-cooperative target in complex space environment. For the sake of deriving a linearized version of the space robot, feedback linearization is used and hence collision avoidance can be formulated as a linear matrix inequality (LMI). The aforementioned model predictive techniques consider the collision avoidance but they lack handling of external disturbances for underactuated systems. In (Johansen et al., 2016), MPC is used for collision avoidance by pre-computing a finite set of control behaviors, and then simulating on-line these behaviors to check which scenario gives the optimal trajectory.

The objective of this paper is to introduce the concept of integrating collision avoidance into the trajectory tracking controller, based on MPC concepts, to act as a last-line of defense for autonomous vessels. For such critical maneuvering, accuracy is necessary and therefore comes the necessity of employing full planar motion nonlinear dynamics and effect of external disturbances. In this paper, a nonlinear state feedback control law is presented based on solving a finite horizon optimization problem, at every instant, and using the current state measurement as initial condition for the problem. The problem takes into consideration the physical constraints of the vessel by systematically adding them to the optimization problem constraints. Collision avoidance constraints are added to the problem that force the vessel to deviate minimally from the defined path in case of predicting a collision while obeying some of the rules of the International Regulations for Preventing Collisions at Sea (COLREGS). External forces are taken into consideration as unmeasured disturbance and therefore the NMPC law is modified to include the disturbance estimated by NDO, and handle the external transverse force component where there is no corresponding control force to counteract. The output of the problem is an optimal sequence, of length N, of the vesselâ€™s force and moment. The first element only is applied and then the whole process is repeated at the next instant. The finite horizon optimization problem is discretized and then formulated as a quadratic problem (QP) which is solved by the aid of ACADO toolkit (Houska et al., 2011) and qpOASES solver (qpOASES Homepage).

This paper is organized as follows. Section 2 describes the vessel nonlinear dynamics, external disturbance modeling, generation of the reference trajectory, and clarifies the control objective. Controller synthesis is presented in Section 3. A brief introduction of NMPC is given first followed by the Nonlinear Disturbance Observer design. A cost function modification is then presented to include sideslip angle; along with the conditions required to guarantee stability of the nonlinear system, collision avoidance, compliance of some COLREGS rules, discretization, and implementation of the proposed approach. The MATLAB based simulation results are given in Section 4. Section 5 concludes this paper.

2. Problem formulation

The surface vessel model has 6-DOF: surge, sway, yaw, heave, roll, and pitch, which can be simplified to motion in surge, sway, and yaw under the following assumptions (Chwa, 2011):

1. The heave, roll, and pitch modes induced by wind and currents are negligible.
2. The inertia, added mass, and hydrodynamic damping matrices are diagonal.
3. The available control variables are surge force and yaw moment.

Based on that, the 3-DOF model will be (Fossen, 2011):

$$
\begin{aligned}
\dot{x} &= u\cos(\psi) - \upsilon\sin(\psi)\\
\dot{y} &= u\sin(\psi) + \upsilon\cos(\psi)\\
\dot{\psi} &= r\\
\dot{u} &= \frac{m_2}{m_1}\upsilon r - \frac{d_1}{m_1}u + \frac{1}{m_1}\tau_u\\
\dot{\upsilon} &= \frac{m_1}{m_2}ur - \frac{d_2}{m_2}\upsilon\\
\dot{r} &= \frac{(m_1-m_2)}{m_3}u\upsilon - \frac{d_3}{m_3}u + \frac{1}{m_3}\tau_r.
\end{aligned} \tag{1}
$$

Here, x and y are the positions, ψ is the heading angle of the ship with respect to the earth-fixed frame, u and υ are the longitudinal and transverse linear velocities in surge (body-fixed x) and sway (body-fixed y) directions respectively, and r is the angular velocity in yaw around body-fixed z axis (see Fig. 1). The parameters m_1, m_2, m_3 are the ship inertia including added mass effects, and d_1, d_2, d_3 are the hydrodynamic damping coefficients.

External environmental forces induced by the wind and wave current are assumed to be constant with respect to the inertial reference frame and have three components; surge, sway, and yaw. Therefore, the vessel model, written in a compact form, will be modified to be:

$$
\dot{\boldsymbol{x}} = f(\boldsymbol{x}) + g_1(\boldsymbol{x})\boldsymbol{u} + g_{2b}(\boldsymbol{x})\boldsymbol{w_b} \tag{2}
$$

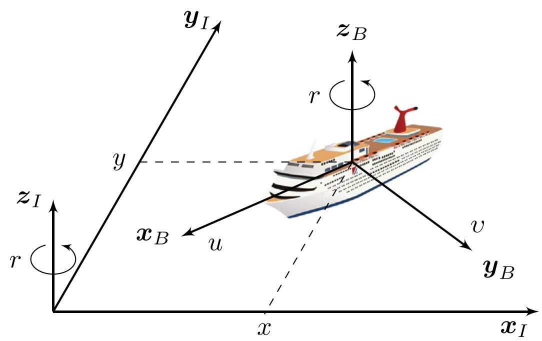

Fig. 1. Earth-fixed (x_I, y_I, z_I) and body-fixed (x_B, y_B, z_B) frames.

where $\boldsymbol{x} = [x\ y\ \psi\ u\ \upsilon\ r]^T \in \Re^6$ is the state vector, $\boldsymbol{u} = [\tau_u \quad \tau_r]^T \in \Re^2$ is the input vector of surge force and yaw moment only, $\boldsymbol{w_b} = [w_u\ w_\upsilon\ w_r]^T \in \Re^3$ is the external forces and moment vector acting on surge, sway, and yaw directions and expressed in the body fixed frame,

$$f(\boldsymbol{x}) = \begin{bmatrix} u\cos(\psi) - \upsilon\sin(\psi) \\ u\sin(\psi) + \upsilon\cos(\psi) \\ r \\ \dfrac{m_2}{m_1}\upsilon r - \dfrac{d_1}{m_1}u \\ \dfrac{m_1}{m_2}ur - \dfrac{d_2}{m_2}\upsilon \\ \dfrac{(m_1 - m_2)}{m_3}u\upsilon - \dfrac{d_3}{m_3}u \end{bmatrix} \in \Re^6,$$

$$g_1(\boldsymbol{x}) = \begin{bmatrix} 0 & 0 & 0 & \frac{1}{m_1} & 0 & 0 \\ 0 & 0 & 0 & 0 & 0 & \frac{1}{m_3} \end{bmatrix}^T \in \Re^6 \times \Re^2, \text{ and}$$

$$g_{2b}(\boldsymbol{x}) = \begin{bmatrix} 0 & 0 & 0 & \frac{1}{m_1} & 0 & 0 \\ 0 & 0 & 0 & 0 & \frac{1}{m_2} & 0 \\ 0 & 0 & 0 & 0 & 0 & \frac{1}{m_3} \end{bmatrix}^T \in \Re^6 \times \Re^3.$$

External environmental forces need to be expressed in the inertial reference frame to be independent from the heading angle of the vessel, therefore the transformation matrix between body and inertial frames will be used as follows (Fossen, 2011):

$$\boldsymbol{w_b} = \begin{bmatrix} \cos(\psi) & \sin(\psi) & 0 \\ -\sin(\psi) & \cos(\psi) & 0 \\ 0 & 0 & 1 \end{bmatrix} \boldsymbol{w}, \boldsymbol{w} \in \Re^3 \tag{3}$$

Here $\boldsymbol{w}$ is the vector of external forces with respect to inertial reference frame. Combining (2) and (3), we obtain the model employed throughout the rest of the paper:

$$\dot{\boldsymbol{x}} = f(\boldsymbol{x}) + g_1(\boldsymbol{x})\boldsymbol{u} + g_2(\boldsymbol{x})\boldsymbol{w} \tag{4}$$

$$\text{where } g_2(\boldsymbol{x}) = \begin{bmatrix} 0 & 0 & 0 & \frac{\cos(\psi)}{m_1} & \frac{-\sin(\psi)}{m_2} & 0 \\ 0 & 0 & 0 & \frac{\sin(\psi)}{m_1} & \frac{\cos(\psi)}{m_2} & 0 \\ 0 & 0 & 0 & 0 & 0 & \frac{1}{m_3} \end{bmatrix}^T.$$

A time-varying reference trajectory is generated by a virtual ship with the same dynamics as (2), but without the effect of external forces:

$$\dot{\boldsymbol{x}}_r = f(\boldsymbol{x}_r) + g_1(\boldsymbol{x}_r)\boldsymbol{u}_r \tag{5}$$

where $\boldsymbol{x}_r = [x_r\ y_r\ \psi_r\ u_r\ \upsilon_r\ r_r]^T$ denotes the generated reference states. The same assumptions as in (Yan and Wang, 2012) are adopted throughout this paper:

Assumption 1: All ship state variables (position, orientation, and velocities) are measurable or can be accurately estimated.
Assumption 2: The reference velocities and positions are smooth over time. Hence, the control objective is to steer the vessel states $(x, y, \psi, u, \upsilon, r)$ to follow the reference states $(x_r, y_r, \psi_r, u_r, \upsilon_r, r_r)$ while satisfying control input and collision avoidance constraints.

3. Controller synthesis

3.1. Nonlinear Model Predictive Control

Consider a continuous time-invariant nonlinear state space model of the vessel in the form of (4) subject to the constraints:

$$\begin{aligned} &\boldsymbol{x}(t) \in \mathscr{X}, \\ &\boldsymbol{u}(t) \in \mathscr{U}, \\ &c(\boldsymbol{x}(t), \boldsymbol{u}(t)) \in \mathscr{C}, t \geq 0, \end{aligned} \tag{6}$$

where $\boldsymbol{x} \in \Re^n$ is the state vector; $\boldsymbol{u} \in \Re^m$ is the control vector; $f(\cdot)$, $g_1(\cdot)$, and $g_2(\cdot)$ are continuous nonlinear functions; $f(0) = 0$, $g_1(0) = 0$, and $g_2(0) = 0$; $\mathscr{X} \subset \Re^n$ and $\mathscr{U} \subset \Re^m$ are compact sets and contain the origin in their interior points. In general, the scheme of MPC is to predict the future states over some finite prediction horizon using a nominal model, as in (4), for the system and the last available measurement or accurate estimation of the states to get the optimum control action over a control horizon (Control Vector). The control horizon is less than or equal to the prediction horizon. This control vector steers the system states to follow a time-varying reference generated by a model of the form (5). Thereafter, the first element of the control vector is applied and the whole process is repeated at the next sample.

Hence, NMPC is considered as a nonlinear state feedback $u(k) = \mathscr{K}(x(k))$ obtained online from an optimal control problem that minimizes a least squares (LS) objective function penalizing the deviation of the system inputs and states from the reference trajectories. It takes the form:

$$\min_{\boldsymbol{x}(t), \boldsymbol{u}(t)} J(\boldsymbol{x}, \boldsymbol{u}) = \int_{t=T_0}^{T_p+T_0} \ell(\boldsymbol{x}(t), \boldsymbol{u}(t))dt + F\big(\boldsymbol{x}(T_p)\big) \tag{7a}$$

subject to :

$$\dot{\boldsymbol{x}}(t) = f(\boldsymbol{x}) + g_1(\boldsymbol{x})\boldsymbol{u} + g_2(\boldsymbol{x})\boldsymbol{w}, \tag{7b}$$

$$\boldsymbol{x}(t) \in \mathscr{X}, \tag{7c}$$

$$\boldsymbol{u}(t) \in \mathscr{U}. \tag{7d}$$

$$c(\boldsymbol{x}(t), \boldsymbol{u}(t)) \in \mathscr{C} \tag{7e}$$

where $\ell(\boldsymbol{x}(t), \boldsymbol{u}(t))$ is the stage cost function and must satisfy the following conditions:

$\bullet \ell(\boldsymbol{x}_r(t), \boldsymbol{u}_r(t)) = 0$

$\bullet \ell(\boldsymbol{x}(t), \boldsymbol{u}(t)) > 0, \forall \boldsymbol{x}(t) \in \mathscr{X}, \boldsymbol{u}(t) \in \mathscr{U}, \boldsymbol{x}(t) \neq \boldsymbol{x}_r(t),$

$F(\boldsymbol{x}(T_p))$ is the terminal cost function, $T_p > 0$ is length of both the prediction and control horizons, and the external disturbance $\boldsymbol{w}$ is known or estimated. The stage and terminal cost functions are usually defined as weighted norm of the states and control input errors (Yang and Zheng, 2014):

$$\ell(\boldsymbol{x}(t), \boldsymbol{u}(t)) = \|\boldsymbol{x}(t) - \boldsymbol{x}_r(t)\|_Q + \|\boldsymbol{u}(t) - \boldsymbol{u}_r(t)\|_R \tag{8}$$

$$F(\boldsymbol{x}(T_p)) = ||\boldsymbol{x}(T_p) - \boldsymbol{x}_r(T_p)||_P \tag{9}$$

Here Q, R, P are positive semidefinite weighing matrices. Control variables are penalized because that makes the optimization problem easier and avoid control values of high energy (Grüne and Pannek, 2011).

3.2. Nonlinear disturbance observer

External environmental forces might lead to a tracking error if they are not considered in the controller design; hence, a measurement or estimation of these disturbances is required. The concept of disturbance observers (DO) was introduced by Ohnishi in 1987 (Nakao et al., 1987). In many control loops, the external disturbances can be modeled by an additive signal added to the control signal (Parsa and Farrokhi, 2010).

In (Fossen, 2000), a nonlinear disturbance observer is designed for vessels under the approximation that $g_2(\boldsymbol{x}) = g_2(\boldsymbol{\psi}) \approx g_2(\boldsymbol{\psi} + \boldsymbol{\psi_w})$, where ψ_w is the wave induced yaw disturbance, which is suitable for the dynamic positioning application presented in that paper. The sway force is estimated in (Aschemann and Rauh, 2010) while the surge and yaw disturbances are compensated using the integral term of the PID. In this subsection, a nonlinear observer is designed to estimate the three components of the disturbances without approximation of the matrix $g_2(\boldsymbol{x})$.

Knowing the disturbance value, it can be compensated by adding an appropriate canceling signal that has the disturbance magnitude but in the opposite sign or equivalently, in the case of MPC, including it in the prediction model. The main idea of disturbance observers is to estimate the equivalent disturbance by comparing the control input to the real system with the virtual control input to the nominal model. The virtual control input is derived from the inverse of the nominal model (Nikoobin and Haghighi, 2009). The estimated value is fed back as a cancellation signal, and then makes the whole system to behave like the nominal system. For vessels, external forces should be estimated as they are not measured in real-time. The combined structure of NMPC with disturbance observer is demonstrated in Fig. 2.

Since the vessel dynamics are highly nonlinear, a nonlinear disturbance observer (NDO), presented in (Chen et al., 2000), is used to estimate the unknown but constant or slowly time-varying external forces. Consider the vessel nonlinear model as in (4), where $\boldsymbol{x} \in \Re^6$, $\boldsymbol{u} \in \Re^2$, and $\boldsymbol{w_b} \in \Re^3$. It is assumed that $f(\boldsymbol{x}),\ g_1(\boldsymbol{x}),$ and $g_2(\boldsymbol{x})$ are smooth in terms of $\boldsymbol{x}$ (Li et al., 2014). To estimate the unknown disturbance, the following disturbance observer is suggested (Li et al., 2014; Chen, 2004):

$$\dot{\boldsymbol{z}} = -l(\boldsymbol{x})[g_2(\boldsymbol{x})z + g_2(\boldsymbol{x})p(\boldsymbol{x}) + f(\boldsymbol{x}) + g_1(\boldsymbol{x})\boldsymbol{u}] \tag{10a}$$

$$\widehat{\boldsymbol{w}} = \boldsymbol{z} + p(\boldsymbol{x}) \tag{10b}$$

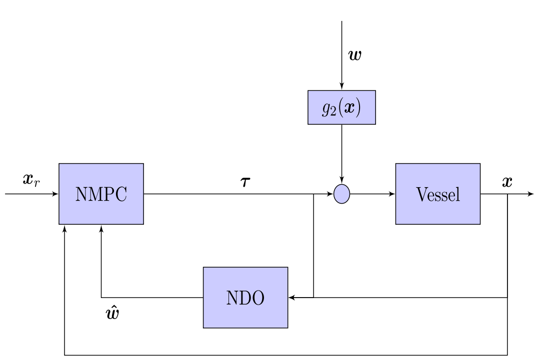

Fig. 2. NMPC-NDO scheme.

where $\boldsymbol{z} \in \Re^3$ is the internal state of the nonlinear observer, and $p(\boldsymbol{x})$ is the nonlinear function to be designed. The nonlinear disturbance observer gain $l(\boldsymbol{x})$ is determined by:

$$l(\boldsymbol{x}) = \frac{\partial p(\boldsymbol{x})}{\partial \boldsymbol{x}} \tag{11}$$

The estimation error is governed according to (Li et al., 2014):

$$\begin{aligned} \dot{\boldsymbol{e}}_w &= \dot{\hat{\boldsymbol{w}}} - \dot{\boldsymbol{w}} \\ &= -l(\boldsymbol{x})g_2(\boldsymbol{x})\boldsymbol{e}_w \end{aligned} \tag{12}$$

Hence, the NDO design can estimate unknown constant disturbances if the observer gain $l(\boldsymbol{x})$ is chosen such that system (12) is asymptotically stable. One possible choice for $l(\boldsymbol{x})$ is:

$$l(\boldsymbol{x}) = K_w g_2(\boldsymbol{x})^{-1} = K_w \begin{bmatrix} 0 & 0 & 0 \\ 0 & 0 & 0 \\ -m_1 u \sin(\psi) & m_1 u \cos(\psi) & 0 \\ -m_2 v \cos(\psi) & -m_2 v \sin(\psi) & 0 \\ m_1 \cos(\psi) & m_1 \sin(\psi) & 0 \\ -m_2 \sin(\psi) & -m_2 \cos(\psi) & 0 \\ 0 & 0 & m_3 \end{bmatrix}^T \tag{13}$$

K_w is a scalar that determines the convergence rate of the observer and $g_2(\boldsymbol{x})^{-1} \in \Re^3 \times \Re^6$ is the pseudo inverse of $g_2(\boldsymbol{x})$. By integrating (11) with respect to $\boldsymbol{x}$, $p(\boldsymbol{x})$ will be:

$$p(\boldsymbol{x}) = \begin{bmatrix} m_1 u \cos(\psi) - m_2 v \sin(\psi) \\ m_1 u \sin(\psi) + m_2 v \cos(\psi) \\ m_3 r \end{bmatrix} \tag{14}$$

This choice makes the observer estimation error linear with eigenvalues equal to the scalar K_w.

3.3. Sideslip angle compensation

In the case of undereducated vessels, the controller can not reject the disturbance force component in the sway direction as there is no sway control force generated by the actuators of the vessel; even if the disturbance value is known.

Although the terms course and heading are used interchangeably in much of the literature on guidance, navigation and control of marine craft (Fossen, 2011), they are not equivalent and this leads to confusion. Here they are going to be used differently, hence the following definitions, adopted from (Fossen, 2011; Breivik and Fossen, 2004), are required to avoid this confusion (see Fig. 3):

Definition 1. **(Velocity Vector).** *It is the specification of the vessels's*

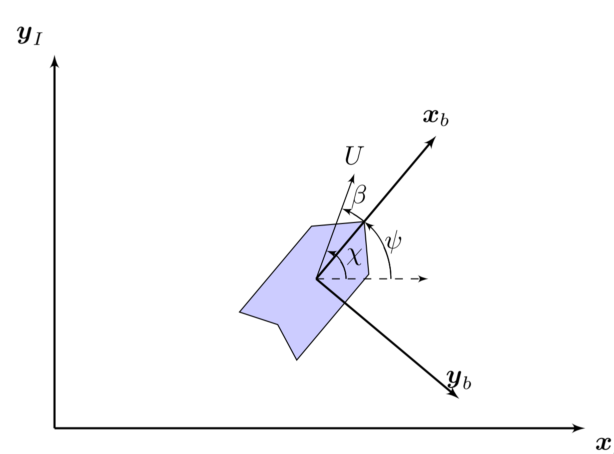

Fig. 3. The geometrical relationship between course χ, heading angle ψ and sideslip angle β.

speed $U = \sqrt{u^2 + v^2}$*, and orientation* $\beta = \tan^{-1}\left(\frac{v}{u}\right)$ *with respect to the vessel's body reference frame.*

Definition 2. **(Sideslip (Drift) Angle β)**. The angle from x_B axis to the velocity vector of the vessel, positive rotation about the z_I axis by the right-hand screw convention.

Definition 3. **(Heading (Yaw) Angle ψ)**. *The angle from* x_I *axis to the* x_B *axis, positive rotation about the* Z_I *axis by the right-hand screw convention.*

Definition 4. **(Course Angle χ)**. *The angle from* x_I *axis to the velocity vector of the vessel, positive rotation about the* z_I *axis by the right-hand screw convention.*

By these definitions, it is clear that $\chi = \psi + \beta$, and in case of straight line motion, the sideslip angle β will be zero and both heading and course angles will be equal except in case of external disturbance acting on the transverse direction. In this case, the sway velocity will not be zero and hence heading and course angle are not equal, even for straight line motion.

In order to overcome the aforementioned limitation due to the absence of sway control force, the heading angle ψ in the stage cost function (8) is going to be replaced with the course angle χ, as the vessel will not be able to achieve zero tracking error for the heading angle in case of external disturbance in the sway direction. This will lead to a non-zero sideslip angle, even if the ship is moving in straight line, but will create a force component that rejects the sway disturbance occurred in the zero-sideslip angle case. Based on that, the control objective will be steering the vessel states to track the reference states except for the heading angle ψ, and the vessel course angle χ to track the reference course angle χ_r where $\chi_r = \psi_r + \beta_r$. Therefore the stage cost function will be modified to:

$$\ell(\boldsymbol{x}(t), \boldsymbol{u}(t)) = ||\overline{\boldsymbol{x}}(t) - \overline{\boldsymbol{x}}_r(t)||_Q + ||\boldsymbol{u}(t) - \boldsymbol{u}_r(t)||_R \tag{15}$$

where $\overline{\boldsymbol{x}} = [x\, y\, \chi\, u\, v\, r]^T$ and $\overline{\boldsymbol{x}}_r(t) = [x_r\, y_r\, \chi_r\, u_r\, v_r\, r_r]^T$. This is motivated by the research done in (Fossen et al., 2014) where sideslip angle is taken into account to cope with high wind and tide conditions and achieve higher tracking accuracy even for smaller ship speeds.

3.4. Collision avoidance

Conventionally, collision avoidance is treated as controller-independent planning problem (Wang et al., 1016). The solution of the problem might not be achievable by the controller due to adverse environmental conditions and ignored vessel dynamics. To overcome that and exploiting the NMPC ability to integrate state constraints systematically into its optimization problem, obstacles are assumed to have circular shape and collision avoidance is translated into an inequality constraint, integrated into the controller design, of the form:

$$\left(x(t) - x_o^i(t)\right)^2 + \left(y(t) - y_o^i(t)\right)^2 \geq R^i \tag{16}$$

where $x(t)$ and $y(t)$ are the prediction of the position for own vessel over the prediction horizon, $x_o^i(t)$ and $y_o^i(t)$ are the prediction of the position for the i^{th} obstacle, and R^i is the safety radius measured from the center of the vessel. The safety radius will be selected to be:

$$R^i = R_o^i + D_s^i + \frac{L}{2} \tag{17}$$

where R_o^i is the radius of the circular envelop for the i^{th} obstacle, L is the length of our vessel, and D_s^i is the safety distance required between the vessel and the i^{th} obstacle. If the obstacle is a ship, the radius of its circular envelope will be selected to be half of its length. Due to lack of information about the encountered vessels acceleration, the assumption of constant velocity is used.

In order to use the above collision avoidance constraint for moving vessels, future motion prediction of encountered vessels is required. It is

Table 1
Surface vessel parameters.

Parameter	Value	Unit
m_1	120.0×10^3	kg
m_2	172.9×10^3	kg
m_3	636.0×10^5	kg
d_1	215.0×10^2	$kg{\cdot}s^{-1}$
d_2	97.0×10^3	$kg{\cdot}s^{-1}$
d_3	802.0×10^4	$kg{\cdot}m^2{\cdot}s^{-1}$

Table 2
States and Control variables weights.

Variable	Weight
X	5
Y	5
X	5
U	1
Υ	1
R	1
τ_u	0.001
τ_r	0.001

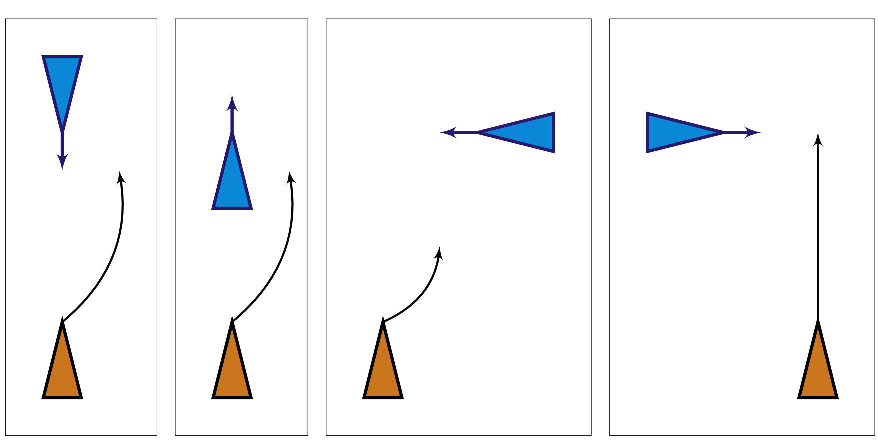

(a) Head-on (b) Overtaking (c) Crossing from the right (d) Crossing from the left

Fig. 4. COLREGS maneuvers for different situations.

assumed that own vessel is equipped with a radar or LiDAR that provides the controller with the position of the obstacles, as well as an AIS/ARPA system that provides necessary information such as velocity, course, and the length of the vessel. The motion prediction of encountered vessels will be predicted using the constant velocity (CV) model presented in (Rong Li and Jilkov, 2003). In this model, the vessel is assumed to move in straight line with constant velocity. The direction of motion is used as the course angle of the vessel χ. It takes the form:

$$\overline{\mathbf{x}}(t)=\begin{bmatrix} x(T_0)+\dot{x}\cdot\Delta t \\ y(T_0)+\dot{y}\cdot\Delta t \\ \arctan\left(\dfrac{\dot{y}}{\dot{x}}\right) \\ \dot{x}(T_0) \\ \dot{y}(T_0) \\ 0 \end{bmatrix}, T_0 \leq t \leq T_p \tag{18}$$

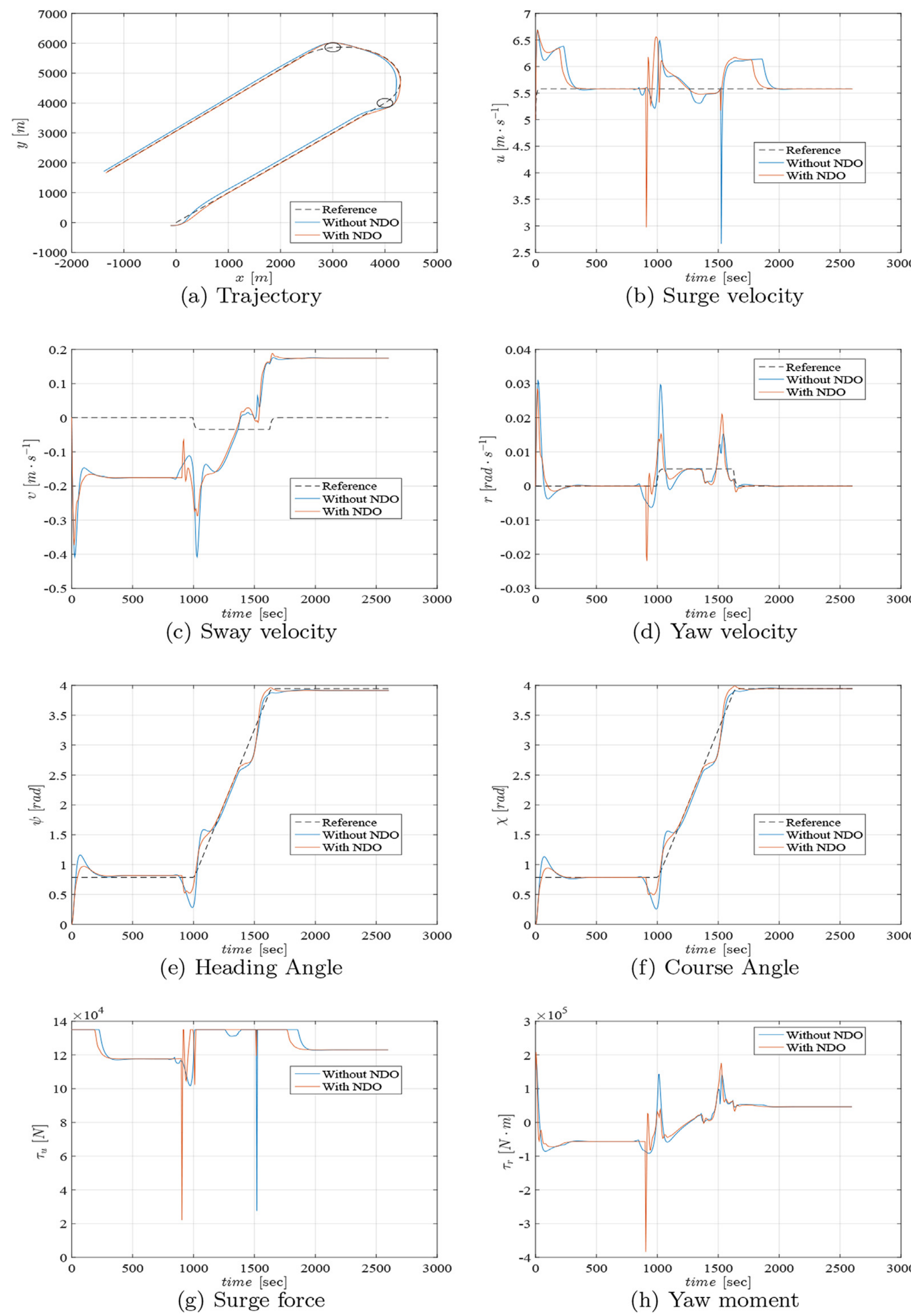

Fig. 5. Simulation results for scenario 1.

where $\Delta t = t - T_0$.

3.5. COLREGS compliance

The maneuvering, occurred due to the optimal solution of the NMPC problem (7) with the collision avoidance constraint (16) as a state constraint, might be random in the sense of maneuvering direction and not necessarily compliant to the International Regulations for Preventing Collisions at Sea (COLREGS) (COLREGS, 1972) that set rules for the actions a vessel should follow when encountering other vessels at sea. We will focus on the three typical situations; head-on, overtaking, and crossing, which are described in rules number 13,14, and 15 of Section 2 of COLRGES and depicted in Fig. 4. In a head-on situation between two vessels, both vessels must turn to the starboard side so that they pass on the port side of each other. In an overtaking situation, the overtaking vessel can turn to either starboard or port side according to the situation, and starboard is chosen for our algorithm. When two vessels are crossing each other, the vessel which has the other on the starboard side must give way and avoid crossing ahead of her. We here conclude that the vessel should prioritize maneuvering to starboard side. Therefore, the optimization problem will be reformulated by adding a soft constraint on the rate of change of yaw moment to prioritize the ship maneuvering to the starboard side. The final form of the optimization problem used is:

$$\min_{\boldsymbol{x}(t),\boldsymbol{u}(t)} J(\boldsymbol{x},\boldsymbol{u}) = \int_{t=T_0}^{T_p+T_0} \ell(\boldsymbol{x}(t),\boldsymbol{u}(t))dt + F(\boldsymbol{x}(T_p)) \tag{19a}$$

subject to :

$$\dot{\boldsymbol{x}}(t) = f(\boldsymbol{x}) + g_1(\boldsymbol{x})\boldsymbol{u} + g_2(\boldsymbol{x})\widehat{\boldsymbol{w}}, \tag{19b}$$

$$\boldsymbol{u}(t) \in \mathscr{U}. \tag{19c}$$

$$\left(x(t) - x_o^i(t)\right)^2 + \left(y(t) - y_o^i(t)\right)^2 \geq R^i \tag{19d}$$

$$\dot{\tau}_r - slk < 0 \tag{19e}$$

$$slk > 0 \tag{19f}$$

where slk is a positive slack variable used for softening the constraint (19e) to give priority to negative yaw moment, i.e. turning to starboard, $\tau_{u,min}$ and $\tau_{u,max}$ are the minimum and maximum limits for surge force, and $\tau_{r,min}$ and $\tau_{r,max}$ are the minimum and maximum limits for sway moment. The stage cost function will be modified to add penalty on the slack variable as follows:

$$\ell(\boldsymbol{x}(t),\boldsymbol{u}(t)) = ||\boldsymbol{x}(t) - \boldsymbol{x}_r(t)||_Q + ||\boldsymbol{u}(t) - \boldsymbol{u}_r(t)||_R + ||slk(t)||_S \tag{20}$$

3.6. Stability of NMPC

To guarantee asymptotic stability by using the control law $u(k) = \mathscr{K}(x(k))$, it is desirable to use infinite prediction and control horizons, i.e., set $N = \infty$ in (7), but it is not feasible to get the solution of the infinite horizon nonlinear optimization problem (Magni et al., 2001). On the other hand, stability can be guaranteed for finite horizon problems by suitably choosing a terminal cost F and a terminal attractive region Ω. This result has been studied in (Magni et al., 2001; Mayne et al., 2000; Ong et al., 2006; Chen and Allgöwer, 1998) and conditions required for that will be summarized as follow:

1 $\mathscr{U}\subset\Re^m$ is compact, and $\mathscr{X}\subset\Re^n$ is connected and contains the origin in the interior of $\mathscr{U}\times\mathscr{X}$.
2 The vector field $f:\Re^n\times\Re^m\rightarrow\Re^n$ is locally Lipschitz in $\boldsymbol{x}$, and satisfy $f(0,0) = 0$.
3 The aforementioned conditions on ℓ are satisfied
4 The terminal penalty F is continuous with $F(0) = 0$, and the terminal attractive region satisfies $\Omega := \{\boldsymbol{x}\in\mathscr{X}|f(\boldsymbol{x})\leq e\}$ for some $e > 0$.
5 The NMPC problem has initially a feasible solution.
6 For any $x\in\Omega$ there exists a $u\in\mathscr{U}$, such that $\frac{\partial F}{\partial x}f(x, u) + \ell(x, u) \leq 0.\forall z\in\Omega$.

For our problem, the constraints on the states are only for the position, so, without loss of generality, we can assume that the feasible set has always the origin in the interior by simple axis transformation. Control constraints are usually selected to be linear inequalities, as shown in (21), and therefore the set $\mathscr{U}$ is compact. Although there are clear conditions for the asymptotic stability, designing the terminal cost F and the attractive region Ω is still an open problem and may make the online optimizations more difficult and time consuming to solve (Jadbabaie and Hauser, 2005). In (Grüne and Pannek, 2011), it was shown that asymptomatic stability can be guaranteed just by tuning P, Q, and R. Closed loop stability is achieved for relatively long horizons without the need to use terminal cost or terminal constraint (Jadbabaie and Hauser, 2005). Based on that, cost function (7) with ℓ selected as in (15) will be used in this paper and without a terminal constraint.

3.7. Direct multiple shooting

In order to solve the optimization problem (7), a direct multiple shooting technique (Bock and Plitt, 1984), derived from the solution of boundary value problems of differential equations, is used. The concept of this technique is based on uniform discretization of the horizon into N smaller intervals using one of the Rungeâ€“Kutta methods such that $t_0 = T_0 < t1 < \cdots < T_N = Tp$, solving an initial value problem in each of the smaller intervals $[t_j, t_{j+1}]$, and imposing additional matching conditions to form a solution on the whole horizon. All Rungeâ€“Kutta variants provide first- and second-order differentiation techniques in order to compute sensitivities of the state trajectory with respect to initial states and control inputs. Other integrators are used in case of algebraic differential equations. Thereafter, the problem constraints are evaluated on the grid nodes t_j and the control vector has been parametrized as piecewise constant. The result of this technique is a least-squares nonlinear programming (NLP) with fixed dimensions that can be solved employing Gauss-Newton method.

The NDO equation (10) is discretized at a sampling interval $T_s = \frac{T_p}{N}$ using Radau IIA fifth-order implicit method, one of Runge-Kutta methods for numerical solution of the ordinary differential equation. This discrete model will be used for estimating the current value of the external disturbance that is assumed to be constant over the NMPC horizon of N elements.

Based on that, The NMPC-NDO scheme is summarized as follow:

1 Set the time index $t = T_0$, the prediction horizon T_p, sampling interval T_s, weight matrices Q and R, the observer convergence rate K_w, and the disturbance initial value $\widehat{\boldsymbol{w}}(T_0) = 0$.

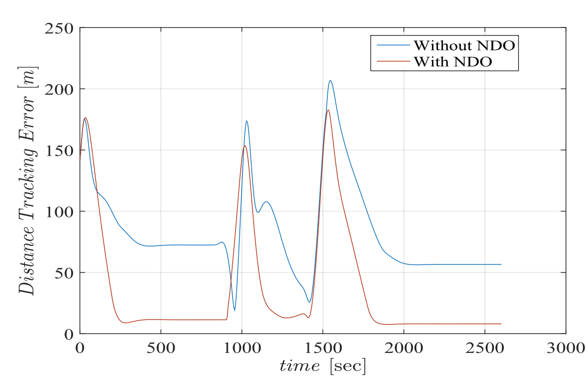

Fig. 6. Distance tracking error using both schemes for scenario 1.

2 Get the value of the states $\boldsymbol{x}$.
3 Get the obstacles position x_o^i and y_o^i.
4 Solve the optimization problem (7), and get optimal input vector $[\boldsymbol{u}(t_0)\cdots\boldsymbol{u}(t_N)]$ and the predicted states $[\boldsymbol{x}(t_0)\cdots\boldsymbol{x}(t_N)]$.
5 Apply only the first element $\boldsymbol{u}(t_0)$.
6 Solve the NDO (10) to get the estimated value for the disturbance $\widehat{\boldsymbol{w}}(t+T_s)$
7 Wait for the next sample and set the time index $t = t + T_s$, then go to 2.

3.8. ACADO toolkit

ACADO toolkit (Houska and Joachim, 2014) is used for solving the underlying NMPC problem by generating a highly efficient C-code, used for real time implementation, and MATLAB executable (mex) files, used for simulation with MATLAB. The main steps of the implementation are briefly described as follow:

- The continuous state space model is symbolically defined using C-code or the MATLAB interface, then it is simplified employing

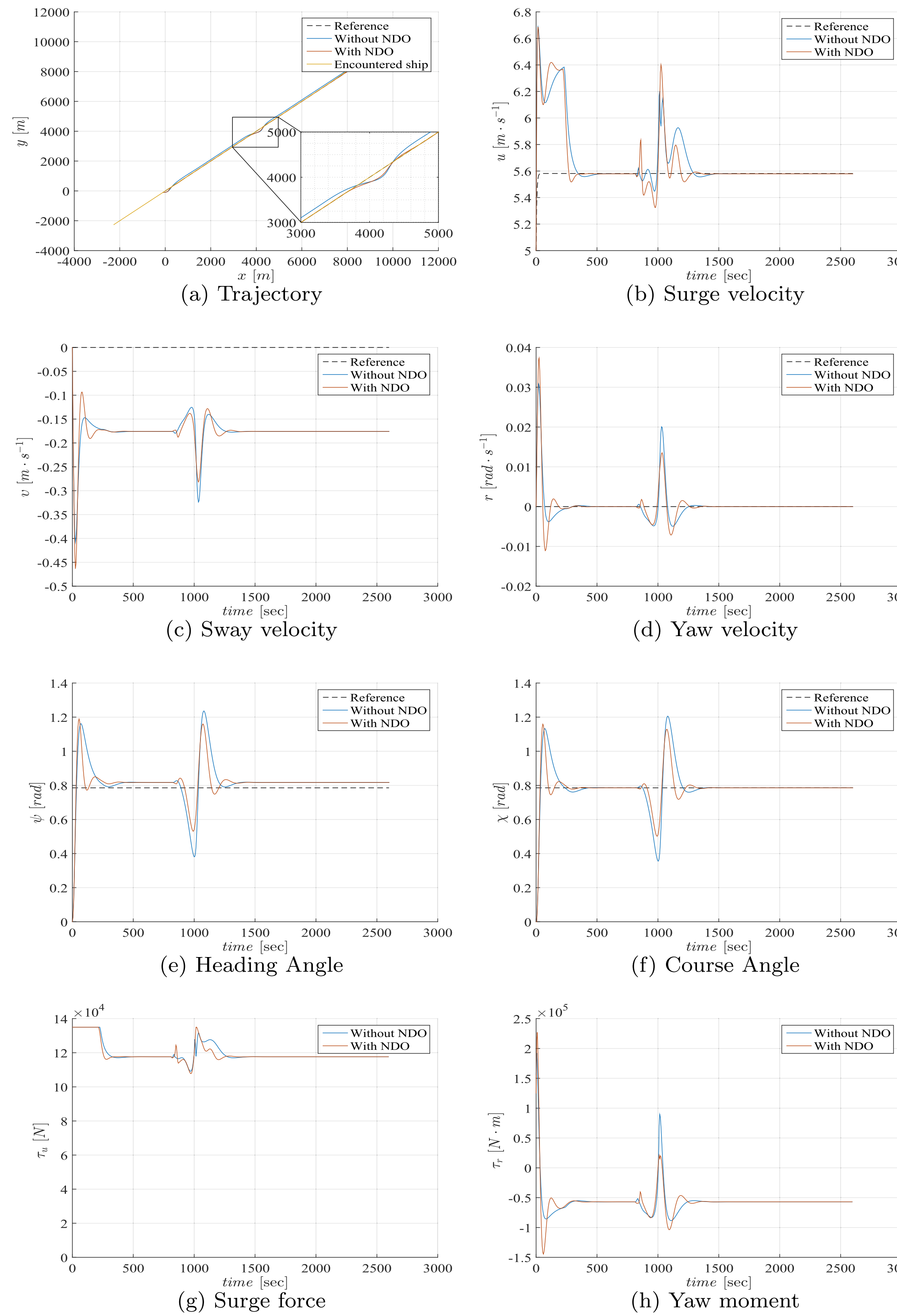

Fig. 7. Simulation results for scenario 2.

automatic differentiation tools and using zero entries in the Jacobian matrix. The result is an efficient real time C-code for the integration of the continuous nonlinear system which will be used for the prediction.

- The optimization problem cost function and constraints are symbolically defined, discretized by the aforementioned direct multiple shooting technique, and the resulting, large but sparse, quadratic problem (QP) is condensed.
- The discretized problem is then passed to a Gauss-Newton iterative algorithm to get a tailored algorithm for solving the underlying QP problem.
- Finally, qpOASES solver, which is designed based on embedded variant of the active-set method, is used to export C-code using fixed dimensions and static memory.

4. Simulation results

In this section, simulation results are presented to demonstrate the validity and assess the performance of the proposed NMPC-NDO scheme for tracking of the underactuated ship (1) with collision avoidance and under the disturbance of external forces. Simulation is done on MATLAB 2014b with the mex files exported using ACADO toolkit and qpOASES. These results have been obtained on a 3.3 GHz core i5 CPU with 8 GB RAM.

The ship chosen for simulation is a monohull ship with a length of $32m$, a mass of 118×10^3 kg and other parameters calculated by using VEssel RESponse (VERES)—a program that calculates the added mass and damping matrices for surface ships, as in Table 1 (Do et al., 2002). The prediction horizon length is selected to be $T_p = 200s$ and the sampling interval is selected to be $T_s = 5$, which both lead to a discrete horizon of $N = 40$ samples. The matrices Q and R are chosen to be diagonal to weight each state and control law independently with the values given in Table 2. The NDO convergence rate is chosen to be $K_w = 0.1$ and the external disturbances with respect to inertial frame are $\boldsymbol{w} = [11\,kN \quad -10\,kN \quad 5\,kN.m]^T$.

Four different scenarios are presented to assess the proposed technique. The first one considers static obstacles, and other three consider the typical collision situations; head-on, overtaking, and crossing. In all of them, own vessel has a straight line reference trajectory and its initial condition is $\boldsymbol{x}(0) = [-100 \ -100\ 0\ 5\ 0\ 0]^T$. The reference trajectory is generated by the reference model (5) using the initial condition $\boldsymbol{x}_r(0) = \begin{bmatrix}0 & 0\,\frac{\pi}{4} & 5 & 0 & 0\end{bmatrix}^T$. The constraints for the surge force and yaw moment are chosen to guarantee the compactness of $\mathscr{U}$ as follow:

$$0.0\,N \le \tau_u \le 135 \times 10^3\,N \tag{21}$$

$$-10.0 \times 10^8\,N{\cdot}m \le \tau_r \le 10.0 \times 10^8\,N{\cdot}m. \tag{22}$$

4.1. Scenario 1

Scenario 1 assess the validity of our approach for avoiding collision with static obstacles. Two obstacles are chosen to be at $(x_o^1, y_o^1) = (4000\,m, 4000\,m)$ and $(x_o^2, y_o^2) = (3000\,m, 5865\,m)$. The radii of the obstacles are assumed to be $R_o^1 = 100\,m$ and $R_o^2 = 100\,m$, and the required safety distances are selected to be 50 m and 50 m respectively. This results in safety radii of $R^1 = 150\,m$ and $R^2 = 150\,m$.

The tracking trajectory of the vessel is presented in Fig. 5a, and the surge, sway, and yaw velocities are presented in Fig. 5b, 5c, and 5d respectively. The surge force and yaw moments are presented in Fig. 5g and h. In the case without NDO, the proposed technique of NMPC can track the trajectory with a small error but using the NMPC-NDO scheme, the vessel can track the desired trajectory with almost zero error. In both cases, collision avoidance constraints, and surge force and yaw moment constraints are respected. It is clear in Fig. 5e and 5f that the heading and course angles are not equal due to the transverse component of the environmental forces, and the controller can not lead to zero tracking error for the heading angle but almost zero for the course angle.

As shown in Fig. 6, the local maximum deviations from the reference trajectory, excluding the transient period at the beginning of the simulation, occur twice while avoiding collision with both obstacles and at which the collision avoidance constraint is active. They correspond to about 169 m and 161 m for the NDO case which are quite acceptable relative to the safety radii of 150 m, and about 207 m and 173 m for the case of not using the NDO. When the collision avoidance constraint is not active, the maximum deviation for the cases with NDO and without NDO are 1 m and 55 m respectively. For both cases, the physical force and moment constraints are respected.

4.2. Scenario 2

In order to assess the performance of the proposed technique for avoiding collision with dynamic objects, i.e. encountered vessels, another vessel is assumed to confront with own vessel in a head-on situation. This vessel is assumed to have no collision avoidance scheme and its position and velocity are assumed to be measured or exchanged via a communication link. The predicted trajectory is calculated using the constant velocity model (18). The encountered vessel is assumed to have a length of 60 m and safety distance of 40 m. This results in a safety radius $R^1 = 100\,m$.

The tracking trajectory of the vessel is presented in Fig. 7a, and the surge, sway, and yaw velocities are presented in Fig. 7b, c, and 7d respectively. The surge force and yaw moments are presented in Fig. 7g and h. It is shown in Fig. 9 that the trajectory tracking error of the NMPC-NDO scheme is close to zero except during the collision avoidance maneuver which achieve a deviation of about 110 m, which is considered small with respect to the 100 m safety radius. On the other side, the case of not using NDO leads to a distance error of $125m$ and $84m$ while collision constraint is active and not active respectively. In both cases, collision avoidance constraints and, surge force and yaw moment constraints are respected. Regardless of using NDO, the collision avoidance

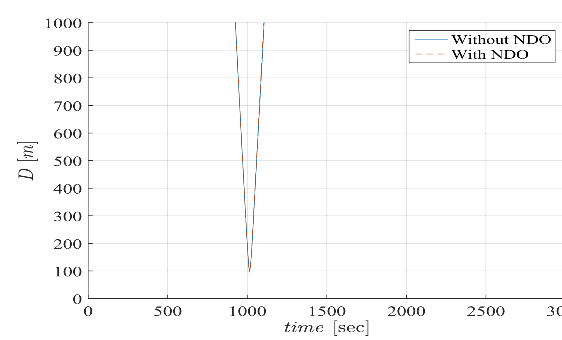

Fig. 8. Distance between the two vessels for scenario 2.

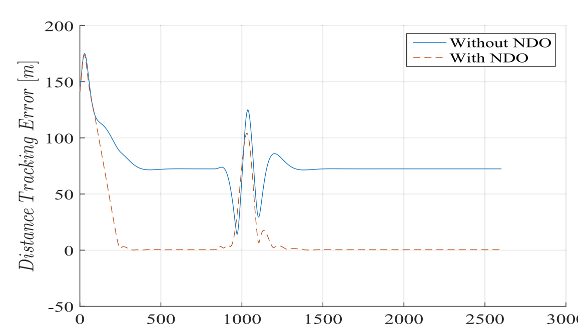

Fig. 9. Distance tracking error of our vessel for scenario 2.

constraint in both schemes leads to a new collision-free trajectory, as close as possible to the reference trajectory. The minimum distance D between the centers of both vessels is about 102 m as shown in Fig. 8, which demonstrates the ability to use our scheme as a last line of defense as this distance is slightly greater than the 100 m safety distance.

4.3. Scenario 3

In this scenario, the overtaking situation is assessed by bringing the encountered vessel on the same path of own vessel but at a lower speed with the same simulation parameters as in scenario 1. As shown in Fig. 10a, own vessel maneuvers to the starboard side, according to rule 13 of COLREGs, then maneuvers back to the original trajectory after overtaking the other vessel. The surge, sway, and yaw velocities are presented in Fig. 10b, c, and 10d respectively, while Fig. 10e and f shows the heading and course angles. In Fig. 10g and h, the surge force and yaw moment generated by our NMPC scheme are shown. The minimum distance D between both vessels is about 105 m.

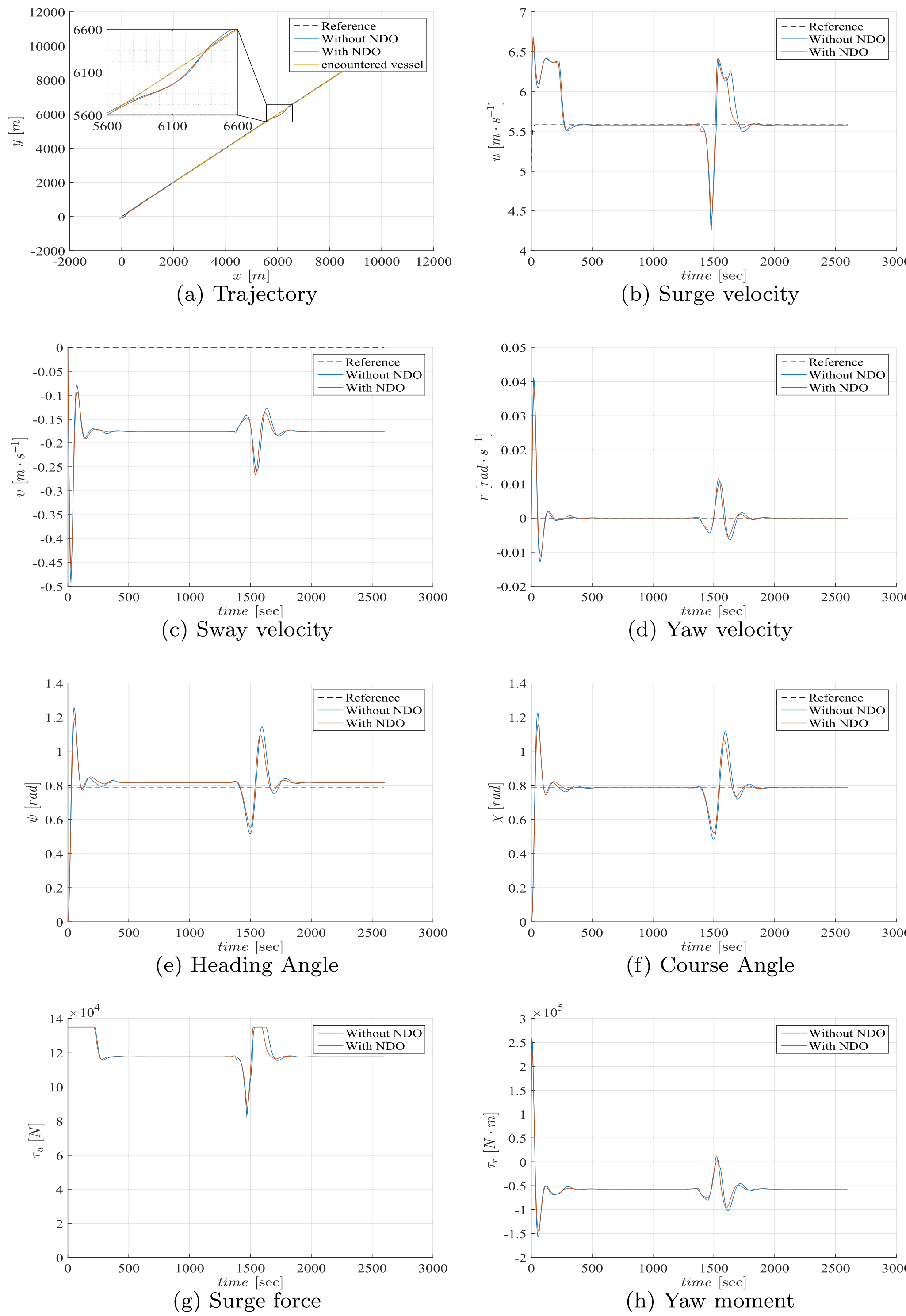

Fig. 10. Simulation results for scenario 3.

4.4. Scenario 4

Scenario 4 tackles the crossing situation where the encountered vessel has path perpendicular to the path of own vessel with a collision designed to occur at the position $(x,y) = (4000m, 4000m)$. Fig. 11 show the states and the control action for this scenario. It is shown in Fig. 11a that own ship obeys rule 15 of COLREGs by turning to the starboard side and passing at aft of the encountered vessel keeping a minimum distance D of about 115 m and then tracks the generated trajectory when the collision risk is over.

As the NMPC scheme does not have an integrator action and relies on the model for the calculating the control action, tracking error is inevitable due to external disturbances and model uncertainty. The NDO will estimate external disturbances and will act as an integrator for the control law. As the vessel starts from an initial condition different from the reference in both scenarios, the surge speed deviates the reference until the position error approaches zero, which is achieved by increasing the position factors of the weighing matrix Q over the velocity factors. This speed deviation happens also in case of collision risk due to the collision avoidance maneuver. The worst-case execution time of the generated

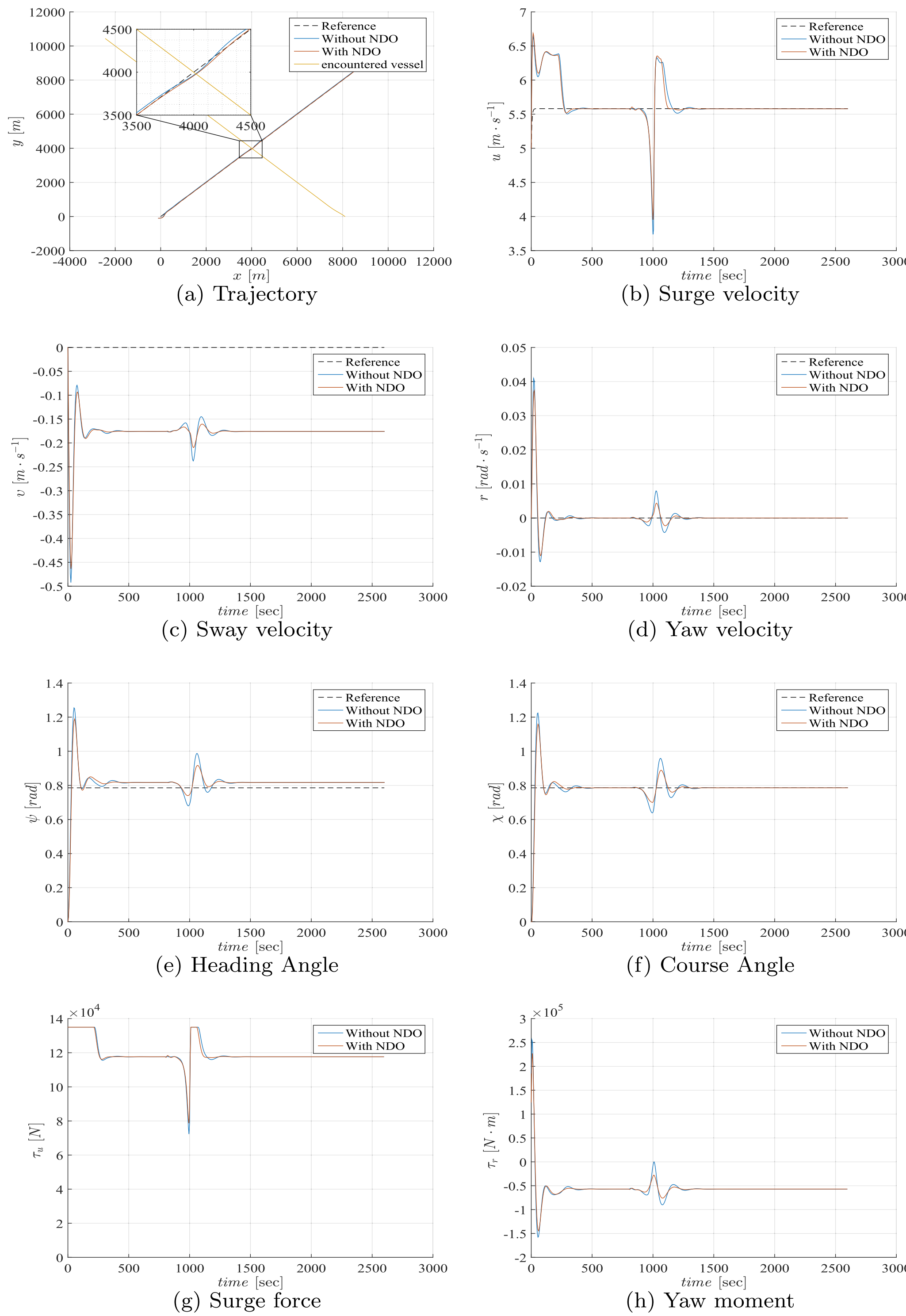

Fig. 11. Simulation results for scenario 4.

code on the aforementioned computer is about 4 ms, which is extremely small compared to the 5.0 s sampling interval and facilitates implementation of the algorithm in real time.

5. Conclusion

A robust NMPC scheme is presented for tracking of underactuated surface vessels with an integrated collisions avoidance technique. A 3-DOF model is used with only two control variables; surge force and yaw moment. Employing a quadratic cost function, real-time efficient C code is generated using the ACADO toolkit and qpOASES solver with collision avoidance as an inequality constraints for the optimization problem. These constraints can handle both static and dynamic objects by satisfying the distance constraint between the predicted position of both the vessel and the obstacle over the horizon. A mex file version of the code is called by MATLAB at each sampling interval to obtain the results. External forces are modeled as unmeasured disturbances and are estimated using NDO to be fed into the NMPC prediction model. Simulation results show the ability of the proposed scheme to track both straight line and curved trajectories while satisfying control law constraints, and achieving collision avoidance of encountered static or dynamic objects. Rules 13,14, and 15 of COLREGS are obeyed to avoid random behavior of the solver. The combined NMPC-NDO scheme shows good robustness to external forces that leads to almost zero tracking error. The maximum execution time of the implemented algorithm is less than 4 ms, which amounts to appr. 0.08% of the sampling interval.

Due to the efficient implementation of the optimization routines, future research will aim at implementing that on Oldenburg University's autonomous vessel named Marine Observation Platform for Surfaces (MOPS) that will also include the time-delay and uncertain measurement of nearby objects into the controller synthesis. Including the 3-DOF dynamics in the collision avoidance maneuvering makes the presented approach useful to act as a last line of defense specially in the situation of restricted maneuverability, which will be also considered for future work. It will as well account for a more sophisticated approaches for the prediction of encountered vessels motion.

References

Abdelaal, M., Fränzle, M., Hahn, A., 2015. Nonlinear model predictive control for tracking of underactuated vessels under input constraints. In: 2015 IEEE European Modelling Symposium on Mathematical Modelling and Computer Simulation, pp. 313–318. https://doi.org/10.1109/EMS.2015.85.

Alrifaee, B., Mamaghani, M.G., Abel, D., 2014. Centralized non-convex model predictive control for cooperative collision avoidance of networked vehicles. In: IEEE International Symposium on Intellligent Control (ISIC), pp. 1583–1588.

Ari, I., Aksakalli, V., Aydodu, V., Kum, S., 2013. Optimal ship navigation with safety distance and realistic turn constraints. Eur. J. Operational Res. 229 (3), 707–717. https://doi.org/10.1016/j.ejor.2013.03.022.

Aschemann, H., Rauh, A., 2010. Nonlinear control and disturbance compensation for underactuated ships using extended linearisation techniques. In: IFAC Proceedings Volumes (IFAC-papersonline), IFAC, Rostock-warnemünde, pp. 167–172. https://doi.org/10.3182/20100915-3-DE-3008.00062. https://doi.org/10.3182/20100915-3-DE-3008.00062.

Bock, H.G., Plitt, K.J., 1984. A multiple shooting algorithm for direct solution of optimal control problems. In: Proc. IFAC World Congress Budapest, pp. 243–247. Budapest.

Breivik, M., Fossen, T., 2004. Path following of straight lines and circles for marine surface vessels. Proc. IFAC CAMS 65–70.

Chen, W.-H., 2004. Disturbance observer based control for nonlinear systems. IEEE/ASME Trans. Mechatronics 9 (4), 706–710. https://doi.org/10.1109/TMECH.2004.839034.

Chen, H., Allgöwer, F., 1998. A quasi-infinite horizon nonlinear model predictive control scheme with guaranteed stability. Automatica 34 (10), 1205–1217.

Chen, W.-H., Ballance, D.J., Gawthrop, P.J., O'Reilly, J., 2000. A nonlinear disturbance observer for robotic manipulators. IEEE Trans. Industrial Electron. 47 (4), 932–938. https://doi.org/10.1109/41.857974.

Chwa, D., 2011. Global tracking control of underactuated ships with input and velocity constraints using dynamic surface control method. IEEE Trans. Control Syst. Technol. 19 (6), 1357–1370. https://doi.org/10.1109/TCST.2010.2090526.

COLREGS, 1972. International Regulations for preventing collisions at Sea. Convention Int. Regul. Prev. Collisions A. T. Sea 1972, 1–74.

Do, K.D., Pan, J., 2004. State- and output-feedback robust path-following controllers for underactuated ships using Serret-Frenet frame. Ocean. Eng. 31 (5–6), 587–613. https://doi.org/10.1016/j.oceaneng.2003.08.006.

Do, K.D., Jiang, Z.P., Pan, J., 2002. Universal controllers for stabilization and tracking of underactuated ships. Syst. Control Lett. 47 (4), 299–317. https://doi.org/10.1016/S0167-6911(02)00214-1.

Dong, Z., Wan, L., Li, Y., Liu, T., Zhang, G., 2015. Trajectory tracking control of underactuated USV based on modified backstepping approach. Iternational J. Nav. Archit. ocean Eng. 7 (5), 817–832.

Fossen, T.I., 2000. Nonlinear passive control and observer design for ships. https://doi.org/10.4173/mic.2000.3.1.

Fossen, T.I., 2011. Handbook of Marine Craft Hydrodynamics and Motion Control, 1st Edition, No. 1. John Wiley & Sons Ltd. https://doi.org/10.1002/9781119994138.

Fossen, T.I., Pettersen, K.Y., Galeazzi, R., 2014. Line-of-Sight path following for dubins paths with adaptive sideslip compensation of drift forces. IEEE Trans. Control Syst. Technol. 23, 820–827. https://doi.org/10.1109/TCST.2014.2338354.

Grüne, L., Pannek, J., 2011. Nonlinear Model Predictive Control Theory and Algorithms. Springer.

Guerreiro, B.J., Silvestre, C., Cunha, R., Pascoal, A., 2014. Trajectory tracking nonlinear model predictive control for autonomous surface craft. IEEE Transaction Control Syst. Technol. 22 (6), 3006–3011.

Houska, B., Joachim, H., 2014. ACADO toolkit User's manual. http://acado.github.io/documentation.html.

Houska, B., Ferreau, H.J., Diehl, M., 2011. ACADO toolkit-An open-source framework for automatic control and dynamic optimization. Optim. Control Appl. Methods 32 (3), 298–312. https://doi.org/10.1002/oca. http://doi.wiley.com/10.1002/oca.939.

Jadbabaie, A., Hauser, J., 2005. On the stability of receding horizon control with a general terminal cost. IEEE Trans. Automatic Control 50 (5), 674–678.

Jiang, Z.P., Nijmeijer, H., 1999. A recursive technique for tracking control of nonholonomic systems in chained form. IEEE Trans. Automatic Control 44 (2), 265–279. https://doi.org/10.1109/9.746253.

Johansen, T.A., Perez, T., Cristofaro, A., 2016. Ship collision avoidance and COLREGS compliance using simulation-based control behavior selection with predictive hazard assessment. IEEE Trans. Intelligent Transp. Syst. 17 (12), 3407–3422. https://doi.org/10.1109/TITS.2016.2551780.

Kahveci, N.E., Ioannou, P. a., 2013. Adaptive steering control for uncertain ship dynamics and stability analysis. Automatica 49 (3), 685–697. https://doi.org/10.1016/j.automatica.2012.11.026. https://doi.org/10.1016/j.automatica.2012.11.026.

Künhe, F., Gomes, J., Fetter, W., 2005. Mobile robot trajectory tracking using model predictive control. In: II IEEE Latin-american Robotics Symposium, pp. 1–7.

Li, S., Yang, J., Chen, W.-H., Chen, X., 2014. Disturbance Observer-based Control :Methods and Applications. Taylor & Francis Group.

Liu, Y.-h., Shi, C.-j., 2005. A fuzzy-neural inference network for ship collision avoidance. In: International Conference on Machine Learning and Cybernetics, pp. 4754–4759. No. 1, Guangzhou.

Magni, L., Nicolao, G.D., Magnani, L., Scattolini, R., 2001. A stabilizing model-based predictive control algorithm for nonlinear systems. Automatica 37 (9), 1351–1362. https://doi.org/10.1016/S0005-1098(01)00083-8.

D. Q. Mayne, Model predictive control: Recent developments and future promise, Automatica doi:10.1016/j.automatica.2014.10.128. URL https://doi.org/10.1016/j.automatica.2014.10.128.

Mayne, D., Rawlings, J., Rao, C., Scokaert, P., 2000. Constrained model predictive control: stability and optimality. Automatica 36, 789–814. https://doi.org/10.1016/S0005-1098(99)00214-9.

Nakao, M., Kouhei, O., Miyachi, K., 1987. A Robust decentralized joint control based on interference estimation. IEEE Proc. Robotics Automation, 1987 Robotics Automation 4 (1987), 326–331. https://doi.org/10.1109/ROBOT.1987.1087996.

Nikoobin, A., Haghighi, R., 2009. Lyapunov-based nonlinear disturbance observer for serial n-link robot manipulators. J. Intelligent Robotic Syst. 55 (2–3), 135–153. https://doi.org/10.1007/s10846-008-9298-2. http://link.springer.com/10.1007/s10846-008-9298-2.

Ong, C., Sui, D., Gilbert, E., 2006. Enlarging the terminal region of nonlinear model predictive control using the support vector machine method. Autom 42 (6), 1011–1016. https://doi.org/10.1016/j.automatica.2006.02.023.

Parsa, M., Farrokhi, M., 2010. Robust Nonlinear Model Predictive trajectory free control of biped robots based on nonlinear disturbance observer. In: 2010 18th Iranian Conference on Electrical Engineering, pp. 617–622. https://doi.org/10.1109/IRANIANCEE.2010.5506996.

Peng, Z.H., Wang, D., Chen, Z.Y., Hu, X.J., Lan, W.Y., 2013. Adaptive dynamic surface control for formations of autonomous surface vehicles with uncertain dynamics. IEEE Trans. Control Syst. Technol. 21 (2), 513–520. https://doi.org/10.1109/Tcst.2011.2181513.

qpOASES Homepage. URL http://www.qpoases.org.

Rong Li, X., Jilkov, V.P., 2003. Survey of maneuvering target tracking. Part I. Dynamic models, Aerospace and Electronic Systems. IEEE Trans. 39 (4), 1333–1364. https://doi.org/10.1109/TAES.2003.1261132. https://doi.org/10.1109/TAES.2003.1261132.

Smierzchalski, R., 1999. Evolutionary trajectory planning of ships in navigation traffic areas. J. Mar. Sci. Technol. 4, 1–6. https://doi.org/10.1007/s007730050001.

Szlapczynski, R., 2011. Evolutionary sets of safe ship trajectories : a new approach to collision avoidance. J. NAVIGATION 64, 169–181. https://doi.org/10.1017/S0373463310000238.

Szlapczynski, R., 2012. Evolutionary sets of safe ship trajectories : evaluation of individuals. Int. J. Mar. Navig. Saf. Sea Transport. 6 (3), 345–353. https://doi.org/10.2478/v10006-012-0074-x.

Szlapczynski, R., Szlapczynska, J., 2012. On evolutionary computing in multi-ship trajectory planning. Appl. Intell. 37, 155–174. https://doi.org/10.1007/s10489-011-0319-7.

Wang, P., Ding, B., 2014. A synthesis approach of distributed model predictive control for homogeneous multi-agent system with collision avoidance. Int. J. Control 87 (1), 52–63. https://doi.org/10.1080/00207179.2013.822100.

M. Wang, J. Luo, U. Walter, A non-linear model predictive controller with obstacle avoidance for a space robot, Adv. Space Res. doi:10.1016/j.asr.2015.06.012.

Wang, H., Wang, D., Peng, Z., 2014. Adaptive dynamic surface control for cooperative path following of marine surface vehicles with input saturation. Nonlinear Dyn. 77 (1), 107–117. https://doi.org/10.1016/j.neucom.2013.11.019.

Wang, T., Yan, X., Wang, Y., Wu, Q., 2017. A distributed model predictive control using virtual field force for multi-ship collision avoidance under COLREGs. In: 2017 4th International Conference on Transportation Information and Safety (ICTIS), Banff, pp. 296–305. https://doi.org/10.1109/ICTIS.2017.8047780. http://ieeexplore.ieee.org/document/8047780/.

Wang, X., Liu, Z., Cai, Y., 2017. The ship maneuverability based collision avoidance dynamic support system in close-quarters situation. Ocean. Eng. (August) 1–12. https://doi.org/10.1016/j.oceaneng.2017.08.034. https://doi.org/10.1016/j.oceaneng.2017.08.034.

Yan, Z., Wang, J., 2012. Model predictive control for tracking of underactuated vessels based on recurrent neural networks. IEEE J. Ocean. Eng. 37 (4), 717–726. https://doi.org/10.1109/JOE.2012.2201797.

Yang, J., Zheng, W.X., 2014. Offset-free nonlinear MPC for mismatched disturbance attenuation with application to a static var compensator. IEEE Transaction Circuits Syst. 61 (1), 49–53.

Zhuo, Y., 2014. Intelligent collision avoidance control for large ships, in: international conference on information science. Electron. Electr. Eng. (ISEEE) 1887–1891. https://doi.org/10.1109/InfoSEEE.2014.6946250.